Cerium: An Unlikely Replacement of Dysprosium in High Performance Nd–Fe–B Permanent Magnets

Arjun K. Pathak, Mahmud Khan, Karl A. Gschneidner Jr., Ralph W. McCallum, Lin Zhou, Kewei Sun, Kevin W. Dennis, Chen Zhou, Frederick E. Pinkerton, Matthew J. Kramer, and Vitalij K. Pecharsky*

Permanent magnets are critical components for numerous devices ranging from electric motors to miniature speakers to disk drives to traction motors for hybrid vehicles to wind generators.[1] The strongest permanent magnets that exist today are based on $Nd_2Fe_{14}B$, which is a complex metallic system. It crystallize in the $P4_2/mnm$ tetragonal crystal structure, where the Nd atoms occupy the 4*f* and 4*g* sites, Fe occupies six different atomic sites (16k_1, 16k_2, 8j_1, 8j_2, 4*e*, 4*c*), and B occupies only 4*g* site.[2,3] $Nd_2Fe_{14}B$ has excellent magnetic properties at room temperature, but poor high temperature performance, and the addition of Dy – a highly critical element[4] – is required for above room temperature applications.[5,6] Rapidly increasing demand for permanent magnets coupled with supply restrictions and the potential for the ever rising costs of critical elements makes a strong economic case for developing competitive magnets that do not rely on critical elements like Dy. Here we report the results of an experimental study performed on Ce (the most abundant and low cost rare-earth element) based $(Nd_{1-x}Ce_x)_2Fe_{14-y}Co_yB$ nanostructured magnets. The intrinsic coercivity (Hci) and maximum energy product ((BH)max) were found to be 17.7 kOe and 12.6 MGOe, respectively for $(Nd_{0.8}Ce_{0.2})_{2.4}Fe_{12}Co_2B$ melt-spun ribbons at T = 300 K. The respective values for hot pressed and die upset magnets of same composition were found to be Hci = 13.7 kOe, (BH)max = 12.8 MGOe, and Hci = 9.4 kOe and (BH)max = 31 MGOe at T = 300 K, respectively. Most importantly, the intrinsic coercivity of $(Nd_{0.8}Ce_{0.2})_{2.4}Fe_{12}Co_2B$ melt spun ribbon and hot pressed magnets is higher than that of 5.9 wt% Dy containing $\{[Nd_{0.45}(Y_{0.66}Dy_{0.33})_{0.55}]_{2.2}Co_{1.5}Fe_{12.5}B\}_{5.58}$ + Ti_2C_2 ribbon[7] (Hci = 11.8 kOe) at 300 K. The value of Hci for $(Nd_{0.8}Ce_{0.2})_{2.4}Fe_{12}Co_2B$ melt spun ribbon and hot pressed magnets at T = 453 K (7.6 kOe for ribbon and 6.9 kOe for hot pressed) is also 49% and 35%, respectively, higher compared to 4 wt% Dy-doped $Nd_2Fe_{14}B$ sintered magnet at $T \geq 450$ K (5.1 kOe at T = 453 K).[8] Our co-doped with Ce and Co $Nd_2Fe_{14}B$ alloy has the highest reported to date intrinsic coercivity at 450 K and above when compared with other Nd–Fe–B based magnets.

Although $Nd_2Fe_{14}B$ and $Ce_2Fe_{14}B$ adopt the same crystal structure, their magnetism is quite different. In $Nd_2Fe_{14}B$, Nd is trivalent, whereas Ce in $Ce_2Fe_{14}B$ is in a homogeneous mixed valence state of 3.44,[9] where the valence fluctuates from +3 to +4 at a frequency $\approx 10^{-13}$ Hz.[10] From empirical alloying theory, a complete solid solution between $Nd_2Fe_{14}B$ and $Ce_2Fe_{14}B$ is expected due to a cell volume difference of only 2.5%. However, as a result of the differences in the Nd and Ce valences, the terminal solid solubility region may end and phase segregation is also possible in $(Nd_{1-x}Ce_x)_2Fe_{14}B$.[11]

The saturation magnetization of $Ce_2Fe_{14}B$ (30.2 μ_B f.u.$^{-1}$) is about 15% lower than that of the corresponding $Nd_2Fe_{14}B$ phase (34.8 μ_B f.u.$^{-1}$), while the Fe moment is only lowered by 2.8% in $Ce_2Fe_{14}B$.[12] The reduction of the Fe moment in $Ce_2Fe_{14}B$ can be ascribed to the hybridization of the Ce 4*f* and Fe 3*d* electrons. In absence of such hybridization (i.e., if Ce is strictly 4^+ and nonmagnetic) we would expect the Fe moment of $Ce_2Fe_{14}B$ to be same as those of the $R_2Fe_{14}B$ (R = La, and Y) compounds where the Fe moments are higher.[12] It is therefore hard to draw a conclusion about the effect of the apparent mixed valence of Ce on the anisotropy and associated permanent magnetic properties of $(Nd_{1-x}Ce_x)_2Fe_{14}B$. Our experimental investigation revealed that the anisotropy and permanent magnetic properties of $(Nd_{1-x}Ce_x)_2Fe_{14-y}Co_yB$ are significantly enhanced but only for a critical concentration of Ce and Co.

The room temperature magnetic hysteresis loop for melt-spun ribbons of pure $Nd_2Fe_{14}B$ is shown in **Figure 1**a, where the intrinsic coercivity (Hci) of 8.4 kOe is observed. As shown in Figure 1b, Hci increases to 10 kOe when 20% of the Nd is replaced by Ce in $(Nd_{1-x}Ce_x)_2Fe_{14}B$ (x = 0.2). With a further increase of the Ce concentration Hci decreases. In addition, the shape of the demagnetization curve in the 2nd quadrant is unfavorably affected (Figure 1c) in the alloys with $0.20 < x \leq 0.30$. Although not shown here, the squareness of the hysteresis loops (B–H) is regained in the alloys with $x > 0.3$. The dependence of Hci, maximum energy product ((BH)max) and

Dr. A. K. Pathak, Dr. M. Khan,[+] Prof. K. A. Gschneidner Jr., Dr. R. W. McCallum, Dr. L. Zhou, K. Sun, Dr. K. W. Dennis, Dr. M. J. Kramer, Prof. V. K. Pecharsky
The Ames Laboratory
U.S. Department of Energy
Iowa State University
Ames, IA 50011–3020, USA
E-mail: cagey@ameslab.gov

Prof. K. A. Gschneidner Jr., Dr. M. J. Kramer, Prof. V. K. Pecharsky
Department of Materials Science and Engineering
Iowa State University
Ames, IA 50011–2300, USA

Dr. C. Zhou
MEDA Engineering and Technical Services LLC
Southfield, MI 48075, USA

Dr. F. E. Pinkerton
General Motors R&D Center
Warren, MI 48090–9055, USA

[+]Present address: Department of Physics, Miami University, Oxford, OH 45056, USA

DOI: 10.1002/adma.201404892

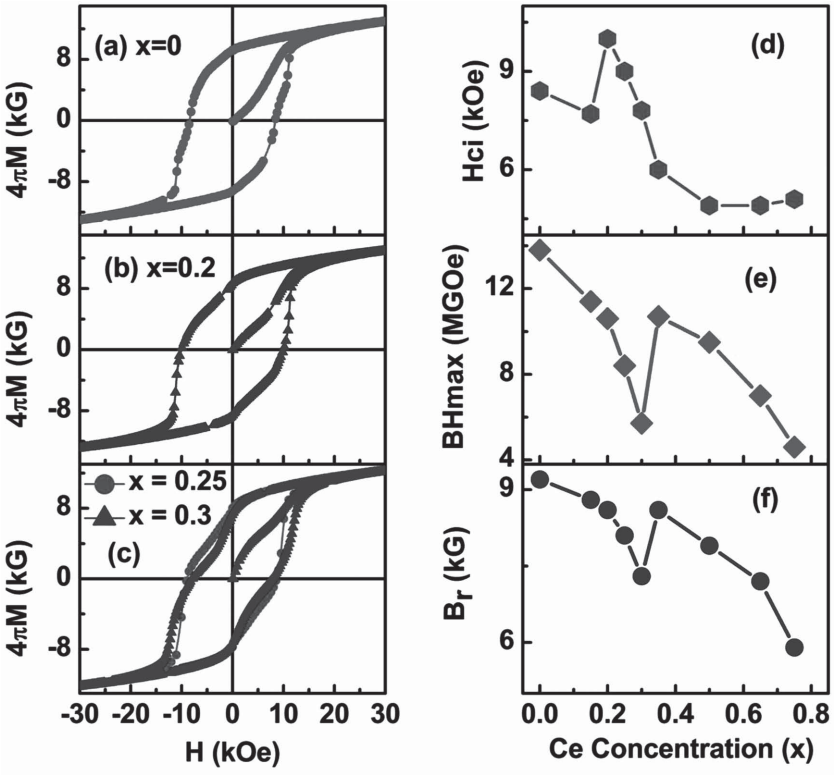

Figure 1. Magnetization measurements of $(Nd_{1-x}Ce_x)_2Fe_{14}B$ melt spun ribbons at 300 K. Magnetization versus magnetic field for a) $x = 0$; b) $x = 0.2$; and c) $x = 0.25$ and 0.3. d) Intrinsic coercivity, Hci; e) maximum energy product, (BH)max; f) remanent magnetization, B_r as a function of Ce concentration (x).

remanence (B_r) on the Ce concentration is shown in Figures 1d, 1e and 1f, respectively. Clearly, Hci is anomalously high, while (BH)max and B_r are anomalously low for the range of concentrations $0.20 \le x \le 0.30$, all of them contradicting the expected (based on the empirical alloying theory and the rule of mixtures) gradual decreasing trends. $(Nd_{1-x}Ce_x)_2Fe_{14}B$ crystallizes in the $P4_2/mnm$ tetragonal crystal structure, and $Nd_2Fe_{14}B$ and $Ce_2Fe_{14}B$ form extensive terminal solid solution regions from $x = 0$ to ≈0.15, and from ≈0.4 to 1 with a phase separated state between $x =$ ≈0.15 and 0.4. The lattice parameters as a function of Ce concentration revealed an anomaly in the tetragonal ***c*** lattice parameter for the samples with x in the vicinity $x = 0.25$.[13] This anomaly is likely to be related to phase separation in the samples with x in the range of $0.20 \le x \le 0.30$, as suggested by the results of the theoretical investigations.[11] The phase separation in this region is also suggested by the scanning electron microscope (SEM) images and from the energy-dispersive X-ray spectroscopy (EDX) analysis, coexistence of $R_2Fe_{14}B$ (R = Nd, Ce) phases that have different concentration ratios of Nd and Ce is evident.[13] We note that our magnetization data for pure $Nd_2Fe_{14}B$ are consistent with that reported in literature.[14] The earlier reported values for pure $Ce_2Fe_{14}B$ are Hci = 5.4 kOe, (BH)max = 4.6 MGOe, B_r = 5.3 kG.[15]

The results depicted in Figure 1 show that the melt-spun ribbons of the Ce doped $(Nd_{1-x}Ce_x)_2Fe_{14}B$ alloys have diminished B_r and (BH)max values. The Curie temperature T_C which was determined from the minima in the first derivative of magnetization with respect to temperature measured in a 1 kOe magnetic field, is also lowered from 580 K for $Nd_2Fe_{14}B$ to 548 K for $(Nd_{0.8}Ce_{0.2})_2Fe_{14}B$. But since the Hci is enhanced for $0.20 \le x \le 0.30$ alloys, Co was substituted for Fe to raise the T_C in the optimally doped compound: $(Nd_{0.8}Ce_{0.2})_2Fe_{14-y}Co_yB$. The maximum energy product (BH)max increases by 50% from 10.6 to 16.0 MGOe for two Co atoms per formula unit substituted for Fe, in addition to increasing T_C by ≈150 to 695 K. The coercivity, which dropped ≈22% from 10 to 7.8 kOe, and the other properties such as anisotropy field, saturation moment, and remanent magnetization remained about the same as the sample without Co addition. A further increase of the Co concentration resulted in a lower (BH)max and Hci, an increased T_C, and essentially no changes in anisotropy field H_A and saturation magnetization M_S. Theoretical calculations have shown that the Co atoms prefer to substituted for Fe in the most favorable Fe(4c) position in the $Nd_2Fe_{14}B$ type structure.[16] The deterioration of the magnetic properties with more than two Co atoms per formula unit in $(Nd_{0.8}Ce_{0.2})_2Fe_{14-y}Co_yB$ may be due to the additional Co atoms occupying other Fe sites.

Figure 2a shows room temperature B–H curves for three differently processed forms of the $(Nd_{0.8}Ce_{0.2})_{2.4}(Fe_{12}Co_2)B$ alloy: rapidly solidified ribbons (sample #1), hot pressed crushed ribbons (sample #2), and die-upset (sample #3). The samples 1 and 2 are isotropic magnets and sample 3 is an anisotropic magnet. At T = 300 K, Hci for samples #1, #2, #3 are 17.7, 13.7, and 9.4 kOe, respectively. Similarly, (BH)max for samples 1 and 2 was found to be almost same ≈12.6 and 12.8 kOe, respectively, and (BH)max for sample 3 was found to be ≈31.2 MGOe at 300 K, which is comparable to recently reported values of (BH)max in sintered magnets that are either more complex than reported here (i.e., contain Ce, Pr, Nd, and Dy),[17] or have an unspecified alloying replacement for Fe.[18] Although, the Hci (at T = 300 K) is the lowest for the die-upset sample (#3), its (BH)max is the largest. This landmark (BH)max value indicates a strong potential for the Nd–Ce–Fe–Co–B alloy to replace many commercial Nd–Dy–Fe–B magnets. We note that following a typical practice in commercially manufactured Nd–Fe–B magnets, an excess of the rare earths has been added to samples #1–#3.

The temperature dependences of Hci (Figure 2b) and (BH)max (Figure 2c) exhibit good high temperature properties. For example, at T = 453 K, the Hci of samples 1 and 2 are 7.6 and 6.9 kOe, respectively, which is higher than 5.1 kOe of 4% Dy doped Nd–Fe–B sintered magnet at the same temperature.[8] Similarly, the (BH)max for samples 1 and 2 are 8.52, and 5 MGOe, respectively at T = 450 K. The Hci and (BH)max for die-upset magnet at T = 450 K are 2.3 kOe and 7.02 MGOe, respectively. It is worthwhile mentioning that the synergistic interactions between Co and $Ce^{3.44+}$ in the rapidly solidified

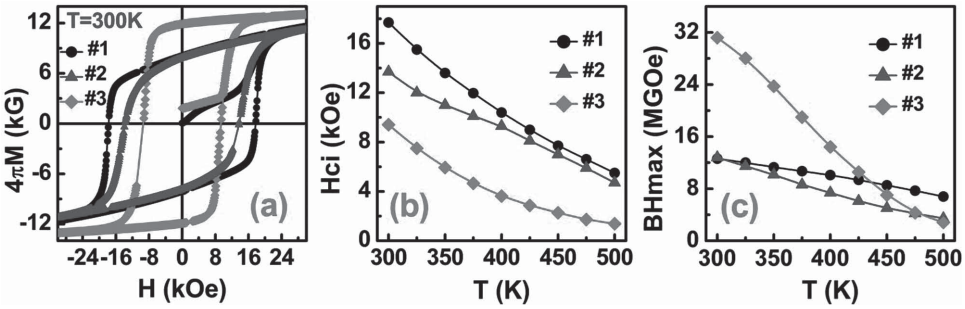

Figure 2. Magnetic properties of $(Nd_{0.8}Ce_{0.2})_{2.4}Fe_{12}Co_2B$ for melt-spun ribbons (#1), hot pressed magnet (#2), and die upset magnet (#3). a) Magnetization versus magnetic field at 300 K; (b) intrinsic coercivity, Hci versus temperature; and (c) maximum energy product, (BH)max versus temperature for melt spun ribbons (#1), hot pressed magnet (#2), and die upset magnet (#3).

ribbons result in smaller slope of the temperature dependence of Hci of the Ce and Co-doped alloy than that Hci of both Dy-Y co-doped NdFeB ribbons,[20] and a Dy, Y, and Co containing NdFeB ribbons.[7] This is important for electric motors used in automotive and other high temperature applications, since Dy is an energy critical element in very short supply.[4]

The high-angle-annular-dark-field (HAADF) scanning transmission electron (STEM) images (**Figure 3**a–c) for samples #1, #2, #3 show brighter contrast along the grain boundaries, indicating segregation of heavy elements. Energy dispersive x-ray spectroscopy (EDS) analysis of sample #2 shows higher amounts of Nd, Ce, and Co on the grain boundary (shown by arrows in Figure 3b), which probably accounts for the excellent magnetic properties shown in Figure 2a–c. Bright-field transmission electron microscopy images show regular equiaxed grains for the isotropic magnet (Figure 3d) and rod-like elongated grains for the die upset specimen (Figure 3e), which is an anisotropic magnet.

We have established that Hci of the rapidly solidify ribbons can be controlled by modifying the chemistry by keeping (BH)max relatively constant. The magnetization measurements for $(Nd_{(1-x)+z}Ce_x)_{2+y}Fe_{12}Co_2B$ + 2.5% ZrC (x = 0.2, y = 0.4, z = 0.16) yield Hci ≈ 18.9 kOe ((BH)max ≈ 15 MGOe) at 300 K; both quantities decrease with increasing temperature to Hci ≈ 6 kOe ((BH)max ≈ 7 MGOe) at 500 K (**Figure 4**a). Hci increases with an increase of excess rare earth up to Ce = 0.48 (i.e., y = 0.4) in $(Nd_{0.8}Ce_{0.2})_{2+y}Fe_{12}Co_2B$ + 2.5% ZrC, and it decreases with a further increase in the Ce concentration (Figure 4b).

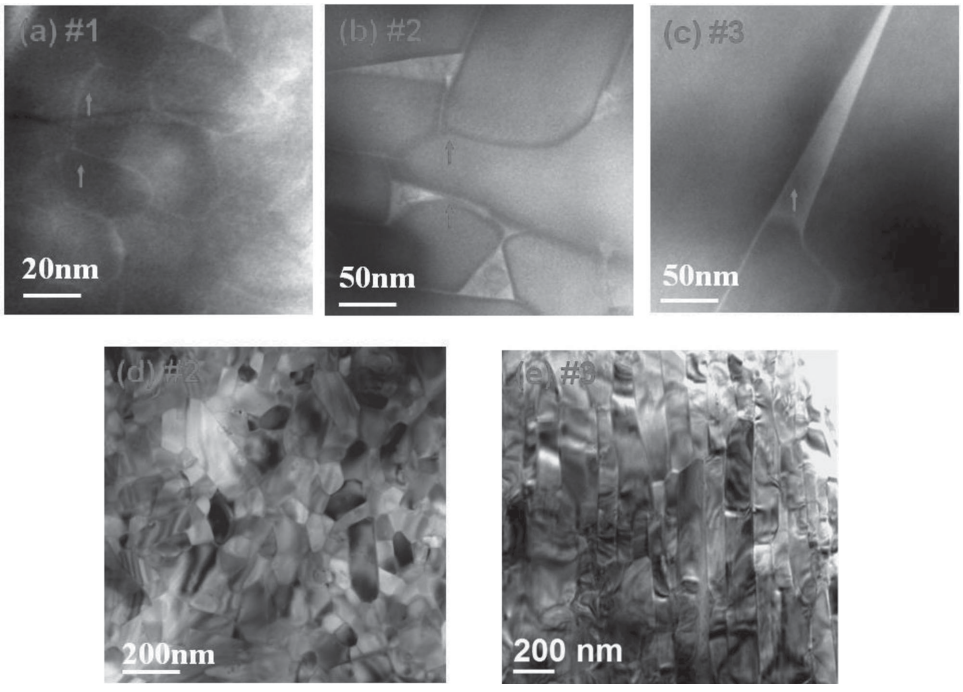

Figure 3. Scanning transmission electron microscopy photomicrographs of $(Nd_{0.8}Ce_{0.2})_{2.4}Fe_{12}Co_2B$ for melt spun ribbons (#1), hot pressed magnet (#2), and die upset magnet (#3). a,b) High-angle-annular-dark-field (HAADF) scanning transmission electron microscopy (STEM) images for samples #1 and #2 showing bright contrast along the grain boundaries, indicating heavy elements segregation. c) HAADF STEM image for die-upset magnet (#3) showing segregation of Nd and Ce at triple junction (shown by arrow). d) Low magnification bright field transmission electron microscopy (TEM) image of sample #2 showing isotropic grains. e) Bright-field TEM image showing elongated grains for die upset magnet (#3).

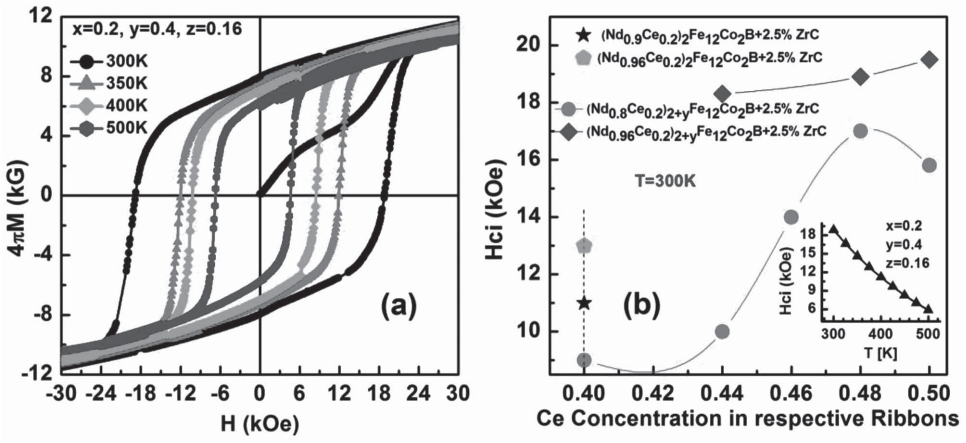

Figure 4. Magnetization measurements of $(Nd_{(1-x)+z}\ Ce_{0.2})_{2+y}Fe_{12}Co_2B$ + 2.5% ZrC melt spun ribbons. a) Magnetization as a function of magnetic field at various temperatures for $(Nd_{(1-x)+z}\ Ce_{0.2})_{2+y}Fe_{12}Co_2B$ + 2.5% ZrC ($x = 0.2$, $y = 0.4$, $z = 0.16$) melt spun ribbon. b) Intrinsic coercivity (Hci) as a function of cerium concentration for $(Nd_{0.8+z}Ce_{0.2})_{2+y}Fe_{12}Co_2B$ + 2.5% ZrC at 300 K. Inset in b) shows Hci as a function of temperature for $x = 0.2$, $y = 0.4$, $z = 0.16$.

The coercivity can be further enhanced by adding extra Nd and making a $(Nd_{(1-x)+z}Ce_x)_{2+y}Fe_{12}Co_2B$ + 2.5% ZrC alloy where $x = 0.2$, $y \geq 0$, and $z > 0$. As shown in Figure 4b, Hci can be enhanced in two different ways: (i) adding more Nd while keeping other constituent elements constant (vertical dashed line), (ii) adding more Ce and Nd to $(Nd_{0.8}Ce_{0.2})_{2+y}Fe_{12}Co_2B$ + 2.5% ZrC (solid circles), and $(Nd_{0.96}Ce_{0.2})_{2+y}Fe_{12}Co_2B$ + 2.5% ZrC (solid diamonds). In both cases, the (BH)max varies from 17.7 MGOe for $(1 - x) + z = 0.96$ and $y = 0$ to 15 MGOe for $(1 - x) + z = 0.8$, and $y > 0$. These values are higher compared to Hci = 11.7 kOe, (BH)max = 11.3 MGOe for 5.9 wt% Dy containing $\{[(Nd_{0.45}(Y_{0.66}Dy_{0.33})_{0.55}]_{2.2}Co_{1.5}Fe_{12.5}B\}_{5.58}$+$Ti_2C_2$ ribbon at 300 K.[7] The temperature coefficient of the coercivity, β (Figure 4b, inset), for $(Nd_{(1-x)+z}Ce_x)_{2+y}Fe_{12}Co_2B$ + 2.5% ZrC is ≈–0.3% °C^{-1}.

Recently, various attempts have been made to reduce the amount of Dy in $Nd_2Fe_{14}B$ magnets. Liu et al.[19] reported that substitution of Y for Dy in $[Nd_{0.8}(Dy_{1-x}Y_x)_{0.2}]_{10}Fe_{84}B_6$ melt-spun alloys decreases Hci and increases (BH)max. The value of Hci and (BH)max for $x = 0.5$ are 7.2 kOe and 17.5 MGOe at 300 K, respectively. The temperature coefficient of Hci (β) for this alloy is –0.394% °C^{-1}. Furthermore, Ce was also substituted for didymium (Di) in $(Di_{1-x}Ce_x)_{27.5}Dy_3Al_{0.1}Cu_{0.1}Fe_{bal}B$ sintered magnet.[20] The magnetic properties (BH)max, Br and Hci decrease. The β varies from –0.64% °C^{-1} for $x = 0$ to –0.55% °C^{-1} for $x = 0.32$, and is nearly twice as large compared to our value of ≈–0.3% °C^{-1}. Overall, the magnetic properties of our best alloys, including β, are substantially better compared to the two alloys noted above.[19,20]

The attractive magnetic properties observed in the $(Nd_{0.8}Ce_{0.2})_{2+y}Fe_{12}Co_2B$ alloys with and without 2.5% ZrC are attributed to a combined effect of Ce and Co. Theoretical calculations show that the Ce^{3+} and Ce^{4+} atoms occupy the Nd(4g), and Nd(4f) sites, respectively[11,16] and the most favored site for Co atom to occupy in the Fe(4c) site.[16] Since the two sites ((Nd(4f) and Fe(4c)) are adjacent to each other, this may account for the synergism between mixed valent Ce and Co, and the enhanced permanent magnet properties. The addition of 2.5% ZrC improves the microstructure of the alloys by enhancing the quenchability while significantly refining the grain size.[7] These microstructural modifications result in even better magnetic properties of the ZrC containing materials.

In conclusion, our study shows that partial co-doping Ce for Nd and Co for Fe results in high strength permanent magnets which are comparable to many of the Dy doped $Nd_2Fe_{14}B$-base grades of permanent magnets. Utilization of these Ce, Co co-doped alloys helps reduce the criticality of Dy-doped alloys[4] by eliminating the need for Dy alloys at least for the lower strength grades, and for high temperatures applications (>450 K), such as the automobile engine compartment and wind turbines. Furthermore, the replacement of 17% to 20% of the Nd (also an energy critical element[4] by Ce (an inexpensive, abundant, noncritical metal) also helps alleviate the Nd shortage. The cost of the components (as of November 2014) of the Ce, Co-doped alloys versus those of Dy based alloys are lower by about 22% to 40%, e.g., \$25.70 per kg for $(Nd_{0.8}Ce_{0.2})_{2.4}Fe_{12}Co_2B$ versus \$33.03 per kg for $Nd_2Fe_{14}B$ + 2%Dy, and \$42.53 per kg for $Nd_2Fe_{14}B$ + 4% Dy. Furthermore, the processing costs of making the sintered $Nd_2Fe_{14}B$ + 4% Dy magnet is much higher than for the die upset $(Nd_{0.8}Ce_{0.2})_{2.4}Fe_{12}Co_2B$ materials, which is significantly higher than the ribbon material of the same composition. Although in the bonded magnets the energy product is reduced to almost 75% of that of the pure unbonded ribbons, the coercivity remains unchanged. Thus, in addition to reducing the criticality of Dy-doped $Nd_2Fe_{14}B$ permanent magnet, the cost of producing Ce, Co-doped alloys is much lower. We do, however, recognize that the new permanent magnet chemistry(ies) reported here will not displace all of the Dy-doped magnets; there are still applications that require very high strength of Nd–Dy–Fe–B magnets.

Experimental Section

Approximately 15 g of stoichiometric $(Nd_{1-x}Ce_x)_2Fe_{14}B$ and $(Nd_{0.8}Ce_{0.2})_{2+y}Fe_{12}Co_2B$ and $(Nd_{(1-x)+z}Ce_x)_{2+y}Fe_{12}Co_2B$ + 2.5% ZrC alloys were prepared by arc melting using Ames Laboratory high purity Nd and Ce. The hot pressed and die upset alloys were made by using commercial grade Ce, Nd metals.[21] In case of the ZrC containing alloys, Zr and C at a concentration equivalent to 2.5 wt% ZrC was added during

the arc melting. The arc melted buttons were then drop-cast into a ≈1 cm diameter ingot for a fine grain size and homogeneous solidification structure throughout the ingot. The melt-spun ribbons were prepared by induction melting the drop-cast alloys in a quartz crucible in 1/3 atm of high purity He gas and then ejected at 125 torr overpressure onto a copper chilled wheel rotating at a tangential speed of 19–25 m s^{-1}. The as-spun ribbons were annealed in He at 600 °C for 20 min (the 600 °C temperature was found to be optimal for the majority of alloy compositions studied). The magnetization measurements were performed using a Quantum Design Inc Physical Property Measurement System (PPMS). Transmission electron microscopy (TEM) samples were prepared by mechanical polishing followed by low voltage short-time Ar ion milling with liquid nitrogen cooling. A FEI Tecnai F20 (200 kV, FEG) TEM was used for microstructural characterization. Six samples, specifically $(Nd_{0.8}Ce_{0.2})_{2.0}Fe_{14}B$, $(Nd_{0.8}Ce_{0.2})_{2.0}Fe_{12}Co_2B$ + 2.5% ZrC, $(Nd_{0.8}Ce_{0.2})_{2.4}Fe_{12}Co_2B$ and $(Nd_{0.8}Ce_{0.2})_{2.4}Fe_{12}Co_2B$ + 2.5% ZrC have been prepared in duplicate to verify reproducibility. The measured magnetic properties (Hci, (BH)max, and Br) are reproducible, with less than 2% difference in all six cases. For example, Hci, (BH)max, and Br for two different samples prepared nominally at the same composition – $(Nd_{0.8}Ce_{0.2})_2Fe_{12}Co_2B$ – are: Hci = 7.83 and 7.84 kOe, (BH)max = 15.10 and 14.82 MGOe (a 2% difference), Br = 8.94 and 8.86 kG (a 1% difference), respectively.

Acknowledgements

This work was supported by the U.S. Department of Energy (DOE), Advanced Research Projects Agency-Energy (ARPA-E), Rare Earth Alternatives in Critical Technologies for Energy (REACT). The research was performed at the Ames Laboratory which is operated for the U.S. DOE by Iowa State University under Contract No. #DE-AC02–07CH11358. The authors would like to thank Chris Celania, Matthew Abben, Matthew Kenney, and Elizabeth Bertelson for their help with preparation of melt spun ribbon samples, and to David Brown at Molycorp Magnequench, Singapore for preparation of hot pressed and die upset magnets.

Received: October 24, 2014
Revised: February 6, 2015
Published online: March 13, 2015

[1] S. Sugimoto, *J. Phys. D: Appl. Phys.* **2011**, *44*, 064001.
[2] J. F. Herbst, J. J. Croat, F. E. Pinkerton, W. B. Yelon, *Phys. Rev. B* **1984**, *29*, 4176.
[3] D. Haskel, J. C. Lang, Z. Islam, A. Cady, G. Srajer, M. van Veenendaal, P. C. Canfield, *Phys. Rev. Lett.* **2005**, *95*, 217207.
[4] Critical Materials Strategy, U. S. Department of Energy, December **2011**.
[5] Ph. Tenaud, H. Lemaire, F. Vial, *J. Magn. Magn. Mater.* **1986**, *101*, 328.
[6] M. Sagawa, S. Fujimura, H. Yamamoto, Y. Matsuura, K. Hiraga, *IEEE Trans. Magn.* **1984**, *20*, 1584.
[7] W. Tang, Y. Q. Wu, K. W. Dennis, M. J. Kramer, I. E. Anderson, R. W. McCallum, *J. Appl. Phys.* **2006**, *99*, 08B510.
[8] T. Akiya, J. Liu, H. Sepehri-Amin, T. Ohkubo, K. Hioki, A. Hattori, K. Hono, *Scr. Mater.* **2014**, *81*, 48.
[9] T. W. Capehart, R. K. Mishra, G. P. Meisner, C. D. Fuerst, J. F. Herbst, *Appl. Phys. Lett.* **1993**, *63*, 3642.
[10] J. Röhler, *Handbook on the Physics and Chemistry of Rare Earths*, (Eds: K. A. Gschneidner Jr., L. Eyring), Vol. *10*, North-Holland Publishing Company, Amsterdam **1987**, p. 453.
[11] A. Alam, M. Khan, R. W. McCallum, D. D. Johnson, *Appl. Phys. Lett.* **2013**, *102*, 042402.
[12] Sinnema, R. J. Radwanski, J. J. M. Franse, D. B. De Mooij, K. H. J. Buschow, *J Magn. Magn. Mater.* **1984**, *44*, 333.
[13] K. A. Gschneidner Jr., M. Khan, R. W. McCallum, V. K. Pecharsky, A. K. Pathak, L. Zhou, D. Brown, F. E. Pinkerton, K. Zhou, in *Proc. 23rd Int. Workshop on Rare Earth and Future Permanent Magnets and Their Applications (REPM* **2014***)*, (Eds: G. C. Hadjipanayis, C. H. Chen, J. P. Liu), Annapolis, Maryland, USA, **2014**, pp. 403–406.
[14] G. Ya. Merkulova, L. Margulies, K. W. Dennis, R. W. McCallum, *J. App. Phys.* **2000**, *87*, 4738.
[15] J. F. Herbst, M. S. Meyer, F. E. Pinkerton, *J. Appl. Phys.* **2012**, *111*, 07A718.
[16] A. Alam, D. D. Johnson, *Phys. Rev. B* **2014**, *89*, 235126.
[17] E. Niu, Z. Chen, G. Chen, Y. Zhao, J. Zhang, X. Rao, B. Ping Hu, Z. Wang, *J. Appl. Phys.* **2014**, *115*, 113912.
[18] M. Zhu, W. Li, J. Wang, L. Zheng, Y. Li, K. Zhang, H. Feng, T. Liu, *IEEE Trans. Magn.* **2014**, *50*, 1000104.
[19] Z. Liu, D. Qian, D. Zeng, *IEEE Trans. Magn.* **2012**, *11*, 2797.
[20] C. Yan, S. Guo, R. Chen, D. Lee, A. Yan, *IEEE Trans. Magn.* **2014**, *50*, 1.
[21] D. N. Brown, Y. K. Lim, R. A. Remoroza, D. J. Miller, *J. Appl. Phys.* **2011**, *109*, 07A742.